LONG-BASELINE, SUB-DECIMETER KINEMATIC GPS POSITIONING OF MOVING OBJECT, WITH POTENTIAL APPLICATION TO MONITOR OCEAN SURFACE WAVE

DR. MOHD EFFENDI BIN DAUD
ASSOC. PROF. KAMALUDIN BIN OMAR
DR. TAJUL ARIFFIN BIN MUSA

FUNDAMENTAL RESEARCH GRANT SCHEME
NO VOTE 0702

UNIVERSITI TUN HUSSEIN ONN MALAYSIA

ACKNOWLEGEMENTS

The research members lead by Dr. Mohd Effendi bin Daud would like to dedicate their sincere thanks to Ministry of High Education (MOHE) for providing the Fundamental Research Grant Scheme (Vot. 0702) for this research work; GNSS & Geodynamics Research Group, Faculty of Geoinformation Science & Engineering, Universiti Teknologi Malaysia.

ABSTRACT

Precise relative kinematic positioning of moving platforms using GPS carrier phase observables has numerous applications. One prominent application is utilization of highly stabilized GPS technology mounted on the buoy, which is specially designed for detecting tsunami wave at open sea. The essential point of this research is to investigate a potential use of a GPS tsunami buoy for the purpose of tsunami early warning system with long-baseline kinematic GPS processing method.

The rule of thumb GPS positioning concept, GPS position results are affected by baseline length mostly due to de-correlation of atmospheric errors. As baseline lengths increase, position results degrade due to the difficulty to correctly fix the carrier phase ambiguity to its integer value. Carrier phase fixed ambiguity solutions are more accurate that float ambiguity solutions. It is generally accepted that carrier phase can be successfully fixed for baselines of up to 10 km. After that, fixing ambiguities becomes more difficult and risky. It would be certainly more advantageous to have a reliable float solution rather than an unreliable fixed solution.

In this study, we have developed a new quasi-real time long-baseline kinematic analysis method using dual-frequency carrier phase with floated ambiguities, implemented in the Bernese GPS Software Version 5.0. We demonstrate that early detection of a damaging tsunami can be achieved by tracking the anomalous changes in sea surface height. The movements of a GPS buoy relative to a base station with baseline length of 500 km have been monitored in quasi-real time mode, and the tsunami waves caused by the 5th September 2004 Off Kii Peninsula earthquake, Japan, have been successful detected as they went by, even though these were only

15 cm high. The filtered record of the solution closely resembles that of short baseline, with RMS of 3.4 cm over 2.5 hours.

To test the robustness of our long-baseline kinematic GPS method under various meteorological, we conducted the GPS tsunami buoy data analysis continuously for 8 days to monitor the motion of the buoy. The average scatterings of GPS buoy heights by the low-pass filtered 1-Hz positioning result after tidal correction are about 3.4 cm and 1.2 cm under both typhoon and calm weather conditions. This accuracy is precise enough to be applicable to a tsunami early warning system. Since our long-baseline kinematic GPS analysis is effective to a long baseline up to 500 km, we can place a GPS buoy far offshore, which ensures an adequate evacuation time even, for people living on the coast.

CONTENTS

LIST OF TABLES

CHAPTER 1

INTRODUCTION

1.1 Background

The precise positioning with GPS of buoys in the deep ocean can be of great help to those studying tides, waves and currents, charting the sea-floor and the marine environment with advanced forms of remote sensing, or calibrating satellite-born altimeters, to map with them the sea surface. To do so in real time may help detect tsunamis far from the coast, giving earlier warning to those at risk. Used with ships, the same technique may enable safer and more efficient marine navigation.

In the deep ocean, potentially devastating tsunami waves (generated by sudden movements of the ocean floor such as earthquakes, landslides, and volcanic explosions) travel at speeds of about 700 km/h as small, gently rising waves of up to 1 m in height. They are hard to detect, because they have periods of 10-30 minutes, and wavelengths of hundreds of kilometers. As they approach the coast, these waves become shorter and higher as the ocean gets shallower. By the time they arrive on shore, they may have become walls of water many meters high, travelling at great speed and causing catastrophic flooding. Tsunami waves are monitored with a combination of land-based tide-gauges and seismometers. In the US, Federal and State government agencies cooperate in the National Tsunami Hazard Mitigation Program (NOAA, 2008). The monitoring devices are located at coastal sites. In order to provide a much earlier warning of an approaching tsunami, NOAA has under way its research project for Deep-ocean Assessment and Reporting of Tsunami (DART), using buoys in the high seas, acoustically linked to sea-floor pressure gauges. The buoys relay the gauge data to a central land site by satellite radio links. If buoys with GPS receivers could be used to monitor short-term changes in mean sea level larger than 10 cm, they could also be used to detect tsunami, possibly at a lower cost.

Another application under study is the use of GPS on buoys to get "ground-truth" observations of mean sea height to validate those from satellite-born altimeters, calibrate those instruments, and correct their biases. Satellite altimetry, primarily a technique for mapping the sea surface repeatedly and worldwide, has proven invaluable for studying ocean currents and tides, climate change, and the Earth's gravity field. Differential, kinematic GPS positioning of buoys relative to nearby coastal stations has been used in the past to study tides and investigate its potential for monitoring sea-level change.

As shown in Figure 1, a running average of the observed instantaneous buoy height, with a window of 5 or 6 minutes duration, largely eliminates the short-term fluctuations due to ordinary waves (with periods of 5 to 30 seconds). This reveals more gradual changes in water level, such as tides and deep-ocean tsunami (Kerr, 2005). The accuracy is a few centimeters. Such accuracy is possible because the differential effect of the ionosphere on the data cancels

itself out on the short baselines used (less than 10 km), making it possible to resolve exactly the carrier phase ambiguities.

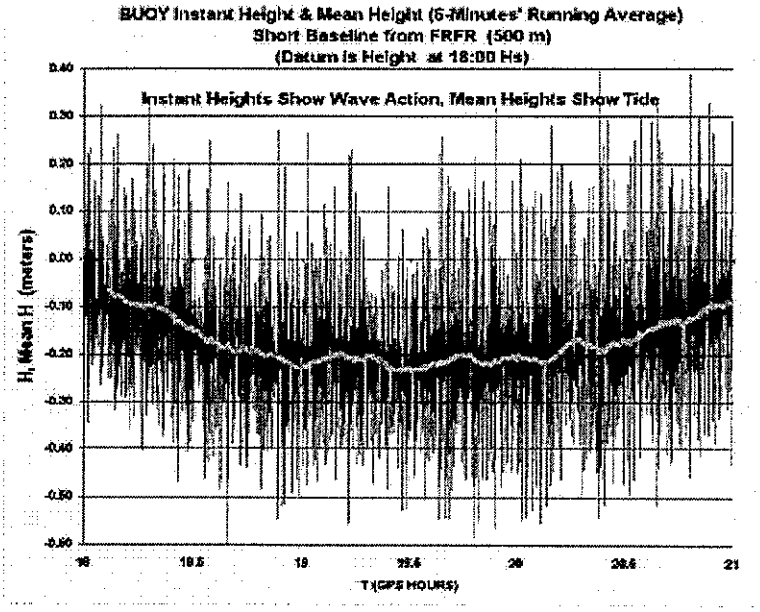

Figure 1: Wave and Tide during test at Duck, North Carolina, as observed with GPS on a buoy. Short-baseline differential solution, with L1 and L2 carrier phase ambiguities resolved.

For deep-sea applications, the buoys can be hundreds and even thousands of kilometers from the nearest land site. The first author has been developing and testing methods for sub-decimeter kinematic positioning over just such long baselines.

1.2 Objectives

The main objective of this research is to produce a strategy of long-baseline kinematic GPS method to monitor a moving object (simulation of moving GPS antenna) to support studies on early warning tsunami system and as a counter measure for disaster mitigation tools. The supportive objectives of this thesis are as follows:

a) to estimate GPS errors from a short, medium and long-baseline kinematic GPS solution,
b) to investigate stability and consistencies of long-baseline kinematic GPS, and
c) to produce the strategy and technique for long-baseline kinematic GPS solution to support an early warning tsunami system.

1.3 Scope of Research

This research aim to develop the strategy of long-baseline kinematic GPS processing to monitor position of buoys placed much farther from shore. As a start, to realize and understand better how to get reliable ans sensitivity of long-baseline (farther from shore) kinematic GPS positioning technique, one GPS experiment or simulation will be conducted in UTHM and UTM (Skudai campus). The experiment will perfome to provide simulation of GPS antenna changing or moving like a buoy floating on sea surface. Here, the GPS antenna of rover station will moving slowly and simultaneously in both direction horizontal and vertical. In addition, the land based GPS stations (reference station or control station) ranging approximately from a few kilometers to more than 100 kilometers from rover station will be establlish to support the experiment. It is suggested the land based GPS stations should be located in UTHM and UTM (Skudai campus).

In summary, this research

- make use of kinematic GPS positioning technique to determine antenna GPS positions rapidly to support disaster mitigation activities.

- explores extension of kinematic GPS positioning technique in real-time mode to monitor sea surface height changes and others applications

- plans toconduct a real application using GPS buoy floating on sea surface.

1.4 Contributions of Research

The contributions of this research primarily consist of four parts. Firstly, contributed to improved studies on tsunami early warning. GPS buoy have been used to detect tsunami wave in the sea, but relatively nearby land site, may arrive to late for timely evacuation measures. In this research, we investigate long-range up to 500km to detect tsunami wave and position of GPS buoy, perhaps give much earlier warning to the coastal populations likely to be affected by tsunami.

Secondly, methodology KGPS processing and results of GPS buoy can be used to determine accurate sea-level on widely differing platforms as long as care is taken to determine the height of the GPS antenna phase center above water level. Applications areas include measuring absolute sea level or temporal variations in sea level and sea level gradient (dominantly the geoid).

Third, the methodology and algorithm of long-baseline KGPS processing for high-rate GPS data as implemented in this study provides another important tools or complement traditional seismology in the study of dynamics earthquake processes at regional and global scale. For example, the most recent application is for ocean-bottom positioning system for monitoring seafloor crustal deformation.

Fourth, this research could be meaning full for oceanographer and navigation purpose. We investigate various fluctuation of sea wave correspond to different weather conditions including typhoon and calm. As the results, they can observe the sea wave height to navigate the boat or vessel and also to issued the warning about the sea wave height. And also they can predict the motion of sea wave.

1.5 Research Report Outline

The remaining parts of the thesis consist of the following 5 chapters:

Chapter 2 is an overview of KGPS positioning model and differential GPS error sources, especially as they relate to the use of a reference receiver. There are included definitions of phase and code errors, double differencing, triple differencing and the errors resulting from various carrier-phase measurement combinations. Each of the differential error sources is then described, including ionospheric, tropospheric, multipath, measurement noise, satellite position error, receiver error, and clock errors. Also we discuss briefly detection of cycle slips and their correction.

Chapter 3 deals with preliminary analysis of KGPS processing within Bernese GPS Software (BSW) version 5.0. We test the performance of KGPS of the GPS buoy data processing method of BSW by processing two sets of GPS data, on-land and marine KGPS. In this chapter we investigate various kinematic processing methods in order to get some idea to develop new processing method for GPS buoy data.

In Chapter 4, a long-baseline KGPS processing strategy was developed. To process GPS buoy data in real time mode, we investigate accuracy of different types of satellite orbit information. We also develop the windowing processing method to allow fully automation processing of GPS buoy data. In this chapter we also briefly describe main program which are used for GPS buoy processing in BSW.

In Chapter 5, result of long baseline KGPS processing for GPS buoy is presented. The GPS buoy data is analyzed during the 5th 2004 Off Kii Peninsula earthquake. This earthquake generated tsunami wave of 20 cm, which is successfully detected from GPS buoy data. Secondly, we discuss the stability and consistencies of long baseline kinematic GPS method. In addition, horizontal movements (horizontal displacements) of GPS buoy on the sea surface is discussed.

We summarize the results and presents recommendations for further research in Chapter 6.

CHAPTER 2

KINEMATIC GPS POSITIONING

The basic idea of kinematic positioning is that the difference of observations between two epochs, collected at the same receiver, to the same satellite equals the change in topocentric range. It does not matter whether the receiver has moved between the epochs, nor does it matter with path the receiver followed to get one point to the other. The integrated carrier phase observable cannot distinguish a moving satellite from a moving receiver antenna. The result of a KGPS survey is the trajectory of the moving antenna with respect to a stationary (reference) site. The antenna of the reference station, remains stationary throughout the kinematic survey. The antenna of another station, called the moving antenna or rover, moves to the points whose positions are to determined (on the ground, in the air, or at sea). Both receivers must continuously track the satellites. Kinematic GPS surveys are possible with pseudo-range, carrier phases, or a combination of both. As a usual case, more accurate positions are derived from the carrier phase observable.

In this chapter we introduce the principle of GPS observation and integration, and to provide

some idea to derived kinematic position. With that in mind, some of the theoretically treatment has been simplified to provide a starting point for a mathematically literate user of GPS who wishes to understand how GPS works, and to get a basic grasp of GPS theory and terminology.

2.1 Models for GPS Positioning

The accuracy of positions depends on the errors in the range measurements scaled by the satellite geometry. The range measurement is obtained by comparing either the PRN (pseudo random noise) code phase or the carrier phase of the received GPS signal with the replica signal generated by the GPS receiver. The observation equation of the GPS code and carrier phase measurements are:

$$P = \rho + d\rho + c(dt - dT) + d_{ion} + d_{trop} + \varepsilon_P \tag{2.1}$$

$$\Phi = \rho + d\rho + c(dt - dT) - d_{ion} + d_{trop} + \varepsilon_\Phi + \lambda N \tag{2.2}$$

where P is the code measurement (m),

ρ is the geometric range from a satellite to a receiver (m),

$d\rho$ is the orbital error (m),

c is the speed of light (m/s),

dt is the satellite clock error (m),

dT is the receiver clock error (m),

d_{ion} is the ionospheric delay (m),

d_{trop} is the tropospheric delay (m),

ε_P is the code multipath error and receiver noise in code measurement,

Φ is the carrier phase measurement (m),

ε_Φ is the carrier phase multipath error and receiver noise in carrier phase measurement (m),

λ is the wavelength of the GPS carrier (m/cycle), and

N is the integer cycle ambiguity (cycle).

In equations 2.1 and 2.2, ρ may be also written as:

$$\rho_r^s = \sqrt{\left(X_r - X^s - \delta X^s\right)^2 + \left(Y_r - Y^s - \delta Y^s\right)^2 + \left(Z_r - Z^s - \delta Z^s\right)^2} \qquad (2.3)$$

where (X_r, Y_r, Z_r) are the coordinates of the receiver antenna,

(X^s, Y^s, Z^s) the coordinates of the satellite, and

$(\delta X^s, \delta Y^s, \delta Z^s)$ the possible errors of satellite coordinates (X^s, Y^s, Z^s).

The usual rule of thumb for a single observer equipped with a GPS receiver reads: by tracking at least four satellites simultaneously, it is possible to solve for the four unknowns (X_r, Y_r, Z_r, dT_r) with an accuracy (comparing the computed and the real position of the observer) of about 10 m for X_r, Y_r, Z_r, and 30 ns for dT_r. The statement holds for a determination of the parameters X_r, Y_r, Z_r, dT_r from a particular estimation model derived from equation 2.2. An estimation model may range from a very simplified version of equation 2.2 to the whole set of equation. The estimation model depends on the type and amount of available information/data and the type of positioning task. Thus, for a single observer performing GPS positioning in real-time, the actual values of some of the parameters in the model are not known, and must therefore be predicted, approximately or even neglected, which leads to the 10 m and 30 ns mentioned above.

2.2 Differential Positioning with GPS

Some of the parameters present in equations 2.2 are spatially correlated. That is the case of ionospheric, tropospheric, and ephemeris modeling parameters. Note also that *dt* the satellite clock error- does not depend on the receiver. If there is an interest in positioning, a usual way to deal with the above parameters is either to approximate them with a priori known data or to cancel them by collecting GPS data simultaneously at close reference point. This is known as differential relative positioning and underlying principle is that both points are affected by nearly the same errors. In formulas, differential relative positioning is carried out by performing the so-

called single or first differences between observations (Wells et al., 1987). First differences for satellite (i) and receivers, say, rover and reference are usually written with the help of the Δ operator:

$$\Delta\Phi = \Phi^{i}_{rover} - \Phi^{i}_{reference} \tag{2.4}$$

where, Φ^{i}_{rover}, $\Phi^{i}_{reference}$ and for any of the expressions of equations 2.2 for *rover and reference*:

$$\Delta\Phi = \Delta\rho + \Delta d\rho + c\Delta dT - \Delta d_{ion} + \Delta d_{trop} + \Delta\varepsilon_{\Phi} + \lambda\Delta N \tag{2.5}$$

Notice that parameters (dt) vanish when single differences between receivers are formed. If the distance between the receivers is small (10-20 km), the single difference ionospheric, tropospheric and ephemeris errors $\left(\Delta d_{ion}, \Delta d_{trop}, \Delta d\rho\right)$ are also small; hence, they can be neglected. In such cases, the integer ambiguities may be easily solved. However, if the distance between receivers is longer, the parameter residuals error cannot be neglected and must be taken into account.

In positioning, most times it is of no interest to solve for the single difference receiver clock error parameter $dT_{1,2} = \left(dT_2 - dT_1\right)$, and so double differences can performed. Double difference observations may be obtained by differentiating two single difference observations, each involving the same pair of receivers but different satellites. Double difference observations, which involve receivers at *rover and reference* and satellites i and j, are expressed with the $\nabla\Delta$ operator, which are basic observables in the Bernese GPS Software Version 5.0 (Hugentobler et al., 2006).

$$\Delta\nabla\Phi = \Delta\Phi^{i} - \Delta\Phi^{j} = \left(\Phi^{i}_{rover} - \Phi^{i}_{reference}\right) - \left(\Phi^{j}_{rover} - \Phi^{j}_{reference}\right) \tag{2.6}$$

Then, after double differencing, equation 2.2 become

$$\Delta\nabla\Phi = \Delta\nabla\rho + \Delta\nabla d\rho - \Delta\nabla d_{ion} + \Delta\nabla d_{trop} + \Delta\nabla\varepsilon_{\Phi} + \lambda\Delta\nabla N \tag{2.7}$$

Performing single or double differences is a particular approach for taking advantages of the high correlation between some parameters in equation 2.2. Rather than eliminating (or gathering)

these auxiliary parameters (receiver time error, instrumental delays, satellite time error, and atmospheric delays), it is possible to estimate them. There are basically two approaches, a global approach and a local one. The global approach makes use of GPS observations spread all over the world as a continuous track of the satellite during the whole orbit, and some receivers are synchronized with an atomic clock. The strength of this observation set makes possible a robust estimation of all the parameters present on the undifferenced equation 2.2. The local approach makes use of external information (precise ephemeredes and precise satellite clocks) to solve the auxiliary parameters present on the undifferenced GPS observation model.

There is a positioning technique called PPP (Precise Point Positioning) based on the undifferenced model where the positioning of a dual frequency GPS receiver is computed using precise ephemeredes and precise satellite clocks. By using PPP and positioning services based on this principle, it is possible to obtain a 10-20 cm precision in position but the lock with the satellites must be maintained for a minimum of 10-20 min to allow the atmospheric parameters to converge (Muellerschoen et al., 2001). This restriction makes these techniques very unstable for kinematic positioning.

The ionosphere, troposphere and receiver clock parameters $(d_{ion}(t), d_{trop}(t), \text{and } dT(t))$ exhibit high temporal correlations. Hence, they can be treated as stochastic parameters in a stochastic dynamics system. In equation 2.7, the term, $\lambda\Delta\nabla N$ is referred to as the double differences ambiguities or the double difference phase integers, and play a key role in geodetic positioning. If these parameters are solved correctly, the phase observations can be considered as highly accurate and precise pseudo-range observations allowing for an accurate and precise kinematic positioning.

The most important feature of the double-difference observation is the cancellation of the large receiver clock error in addition to the cancellation of the large satellite clock errors. These receiver clock errors cancel completely as long as observations to satellite are taken at the same time, or the receiver clock drifts between the observation epochs are negligible. The small clock terms, which are function of the topocentric range rate, remain in equation 2.5. Because multipath is a function of the specific satellite-receiver reflector geometry, it does not cancel in

the double difference observable.

An alternate approach to processing is to formulate triple difference from double difference for the carrier equation. The advantage to this alternate approach is that the integers do not have to be considered. In a similar fashion, any cycle slips, which could be viewed as the introduction of a new integer value, are handled automatically. Before introducing the triple differences, let us combine the two carrier equations into one ionospherically free carrier equation. Notice that we simply multiply one equation by the ratio of frequencies squared and then subtract equations. We modified the equation 2.7, which are involve rover receiver (ro), reference receiver (re) and satellites i, j to make it more easier understanding.

$$\lambda_2(\Phi_2 + N_2)^{i,j}_{ro,re}\frac{f_2^2}{f_1^2} - \lambda_1(\Phi_1 + N_1)^{i,j}_{ro,re} = \left(\rho^{i,j}_{ro,re} + T^{i,j}_{ro,re}\right)\left(\frac{f_2^2}{f_1^2} - 1\right) + (\varepsilon_2)^{i,j}_{ro,re}\frac{f_2^2}{f_1^2} - (\varepsilon_1)^{i,j}_{ro,re} \tag{2.8}$$

where ro, re indicates GPS receivers at rover and reference sites,

i, j indicates GPS satellites i and j,

T represents the path delay caused by the signal traveling through the Atmosphere, and

ε represents carrier phase modeling error (measurement error and multipath).

To achieve the desired final form of these ionospherically free carrier double difference equations we divided through by the parenthetical frequency term and simply the noise term.

$$\frac{\lambda_2(\Phi_2 + N)^{i,j}_{ro,re}\frac{f_2^2}{f_1^2} - \lambda_1(\Phi_1 + N)^{i,j}_{ro,re}}{\left(\frac{f_2^2}{f_1^2} - 1\right)} = \left(\rho^{i,j}_{ro,re} + T^{i,j}_{ro,re}\right) + \varepsilon^{i,j}_{ro,re} \tag{2.9}$$

The later term can be simplified as follows (where the (if) subscripts imply ionospherically free).

$$\left(\Phi_{if}\right)^{i,j}_{ro,re} = \left(\rho^{i,j}_{ro,re} + T^{i,j}_{ro,re}\right) + \varepsilon^{i,j}_{ro,re} \tag{2.10}$$

The tropospheric delay can be expressed as a function of zenith path delay $\Delta_{ro,re}$ and a mapping function $M(E)^{i,j}_{ro,re}$, we get:

$$\left(\Phi_{if}\right)^{i,j}_{ro,re} = \left(\rho^{i,j}_{ro,re} + M(E)^{i,j}_{ro,re}\Delta_{ro,re}\right) + \varepsilon^{i,j}_{ro,re} \tag{2.11}$$

where $E^{i,j}_{ro,re}$ stands for the elevation angles of satellites i and j with respect to receivers at rover and reference stations (strictly speaking, with respect to the local horizon of receivers at rover and reference stations). This is the final form for the ionosphere-free carrier double difference equation. We still must formulate the ionosphere-free carrier triple difference equations by subtracting the ionosphere-free double difference equation at epoch t_1 and t_2. The time difference $t_2 - t_1$ is normally one second. The process of subtracting like double difference from consecutive epochs results in all ambiguities N being eliminated from the formulation.

$$\left(\Delta\Phi_{if}\right)^{i,j}_{ro,re} = \left(\Delta\rho^{i,j}_{ro,re} + \Delta(M(E)^{i,j}_{ro,re}\Delta_{ro,re})\right) + \Delta\varepsilon^{i,j}_{ro,re} \tag{2.12}$$

Assuming phase lock, the initial integer ambiguity N has canceled in equation above. Notice that the triple and double differences have the same sensitivity with regard to clock errors and satellite frequency offset. The triple-difference observable is probably the easiest to deal with because the ambiguity cancels. The triple-difference solution is often considered a pre-processing technique to get good approximate positions for the double difference solution. Triple-difference has a major advantage in that cycle slips are mapped as individual outliers in the computed residuals. Individual outliers can usually be detected and removed or corrected. The resulting cycle slip free (or nearly so) observations can be used in the double difference solution. Tropospheric refraction usually does not change rapidly with time and it is thus considerably reduced on the triple-difference level. This is not true, however, for the ionospheric refraction, which may show very rapid variations in time particularly in high northern and southern latitudes. Table 2.1 is listed the common error cancellation differential techniques.

Table 2.1 Common-mode Cancellation

Observation	Effects eliminated	Effects reduced	Option
Single Difference	first order satellite clock	orbit errors geometric	constraint ambiguity
Double difference	first order satellite & station clocks	position error ionosphere	constraint ambiguity
Triple difference	first order satellite & station clocks	troposphere	ambiguity eliminated

Table 2.2 Linear combination of carrier phases

Signal	*n*	*m*	$\lambda_{n,m}$ cm	V_I	$\sigma_{n,m}$ mm
L1	1	0	19.0	0.779	3.0
L2	0	1	24.4	1.283	3.9
$L_{widelane}$	1	-1	86.2	-1.000	19.4
$L_{narrowlane}$	1	1	10.7	1.000	2.1
$L_{ionfree}$			≈ 5.4	0.000	10.0

2.3 Receiver Clock Synchronization

The term (cdT) in equation 2.2 may be eliminated by forming the differences of the measurements to two satellites. The term (dt) may be eliminated using the differences between two receivers. However, that the receiver clock error (dT) is completely eliminated in the differences. In order to compute the geometric distance between satellite and receiver at time in GPS time scale, the receiver clock error (dT) has to be known only 0.1 μsec accuracy. In fact, if we could determine receiver clock error to 0.1 μsec or smaller yielding error in the geometric distance induced by a receiver clock error will be smaller than 1 mm. Therefore, the observations must be synchronized in a pre-processing step at a higher accuracy level.

To tackle this challenge, we applied pseudorange solution in Bernese GPS Software using smoothing code (zero differences). These solutions allow us to synchronize the clocks, or to determine the receiver clock error to 0.1 μsec. The remaining, unavoidable clock synchronization errors will be neutralized through double differences of the carrier phase observables.

2.4 Cycle Slip Detection/Correction

Another important assumption about the models used in differential positioning with GPS is that data free from cycle slips. A cycle slip occurs when the receiver loses lock with a satellite signal. When a cycle slip is present, the carrier phase ambiguity is no longer a constant and either it must be repaired or a new ambiguity parameter must be determined. If the cycle slip is not identified, equation 2.1 will no longer be true and a systematic error will be present in the trajectory determination.

A cycle slip can be due to several different reasons: obstructions between the antenna and the signal path, high signal noise due to multipath or when signals from a low elevation satellite are received, interference, or receiver signal processing. Cycle slips caused by antenna obstructions are usually very easy to detect because they are a few thousands of cycles wide. However, cycle

slips due to multipath and receiver signal processing can be only 1 or 2 cycles wide and are, therefore very difficult to detect, especially in kinematic operation mode. There are no unique methods for eliminating cycle slips.

One of the various methods for cycle slip fixing is to carry out a triple-difference solution first. Before computing the double difference solution, the double difference observation should be corrected for cycle slips identified from the triple-difference solution. A simple method is to change the weights of those triple-difference observations that have particularly large residuals. Once the least-square solution has converged, the residuals will indicate the size of the cycle slips. In a good solution the residuals are small fractions of a cycle, and only those triple-differences containing cycle slips will have residuals close to one cycle or larger. Since triple-difference processing is not only robust technique for cycle slip detection, it also provides a good solution for the station coordinates, which, in turn, can be used as approximate positions in subsequent double difference solutions.

2.5 GPS Error Sources

Equation 2.5 shows seven different GPS error sources which can be categorized into three different types according to their spatial and temporal correlations:

1). Only satellite correlated: satellite clock error such as (SA) until May 2000,
2). Spatially correlated: satellite orbital error, ionospheric and tropospheric error,
3). Independent error: receiver noise and multipath error.

The first type of errors can be totally removed by single differencing between two receives. The second type of errors can be reduced by single differencing; however, the residual errors increase as the separation increase. The third type of errors cannot be removed by any differencing techniques and they are independent of baseline lengths.

2.5.1 Orbital Error

Orbital error results from the uncertainties in the broadcast ephemeris. These uncertainties are due to the accuracy limitations associated with the predicted nature of the broadcast ephemeris. The orbital error is generally a few metres; but sometimes, it reaches tens of meters due to the problem of orbital prediction (Lichten and Border, 1987). Orbital error can be greatly reduced by differencing between receivers. A more effective way to handle orbital error is to use post-processed precise orbits. Precise orbits are derived from an extensive reference network and the accuracy can be as high as a few centimeters (International GNSS Service, 2008). However, precise orbits are not available for real-time applications.

2.5.2 Ionospheric Error

Ionospheric error is caused by the presence of free electrons when GPS signals pass through the upper layer of the atmosphere. The effect on range may vary from 150 meters (at midday, during periods of maximum sunspot activity, with the satellite near the horizon of the observer) to less than five meters, (at night, during periods of minimum sunspot activity, with the satellite at the zenith) (Wells et al., 1987). For GPS carrier frequencies, the ionospheric delay is dispersive. This fact can be used to advantage, since a special linear combination of the dual-frequency GPS observations can be formed to eliminate most of the ionospheric effect. Ionospheric correction coefficients from the broadcast ephemeris can only remove 50% of the ionospheric delay at mid-latitudes (Wells et al., 1987). Recent research on precise prediction of the ionospheric delay using a wide-area GPS network, such as WASS, or using a regional network (Raquet, 1997), has shown some good results for correcting the ionospheric delay using interpolation or least squares collocation.

2.5.3 Tropospheric Error

Tropospheric delay is caused by the refraction of the GPS signal in the troposphere. The delay contains two parts. The larger part is caused by the dry atmosphere component, which is

stable and predictable. The delay resulting from the water vapor is smaller, but varies greatly. At GPS frequencies, the troposphere is non-dispersive. The tropospheric delay is strongly correlated over a short distance between the reference and the rover stations when the height difference of the two stations is small. However, when the separation or height difference is large, local atmospheric conditions will be different and the correlation becomes weaker. Surface meteorological data is not accurate to adequately represent atmospheric conditions along the signal path (Spilker Jr., 1996). To get more accurate estimations, the water vapor content of the atmosphere along the propagation path can be measured with water vapor radiometers (Resch, 1984). However, the instruments are very elaborate and expensive. Now, GPS networks are also used to predict the relative troposheric wet delay (Zhang, 1999).

2.5.4 Multipath

Multipath occurs when reflected signals, in addition to the direct signal, reach the antenna. It depends highly on the properties of the reflector, the antenna gain pattern, and the type of correlator used in a receiver. Multipath interferes with the correlator in a GPS receiver to precisely determine the time instant of signal reception. It affects both pseudorange and carrier phase measurements. The code multipath is generally much larger than the carrier phase multipath. It can reach up to one-half of a chip length of the PRN code, assuming an environment in which the multipath signal strength never exceeds that of the direct signal (Goldhirsh and Vogel, 1989). By contrast, the carrier phase multipath is always less than one-quarter of the carrier wavelength (Georgiadou and Kleusberg, 1988). Typically, for static observations, multipath is non-Gaussian in nature and shows sinusoidal oscillations with periods of a few minutes due to the change of satellite geometry. In kinematic applications, multipath behaves more randomly because the movement of the rover changes the reflecting geometry in a relatively random way. For most precise positioning applications, multipath is one of the major error sources, because it decorrelates very fast over distance and cannot be reduced by differencing or modeling.

CHAPTER 3

PRELIMINARY ANALYSIS OF CARRIER PHASE DIFFERENTIAL KINEMATIC GPS POSITIONING

3.1 Introduction

The aim of this chapter is to assess the performance of carrier phase differential KGPS positioning using Bernese GPS Software (BSW) Version 5.0. We discuss the performances of KGPS to processed GPS data collected from two different tests on-land and at sea. At the on-land test (hereafter refer as quasi-kinematic test), data were logged at 1-second time interval for the 4 consecutive days. The relationship between daily kinematic solutions and baseline length were investigated. At the marine test, GPS data with a vessel were logged at 1-second time interval. The results expected from both solutions will be used as a preliminary assessment of capability of KGPS solution within BSW. These preliminary assessments become valuable

references for us to develop long-baseline KGPS methodology for GPS buoy data discussed in Chapter 4.

3.2 Data Collection Campaigns

3.2.1 On-land Test

The quasi-kinematic test took place in March, 2010 at the Faculty of Civil and Environmental Engineering, University Tun Hussein Onn Malaysia (UTHM). Data were collected using an Ashtech UZ-12 receiver with an ASH701945_M geodetic antenna. These observations were carried out as one of field test of the studies.

The quasi-kinematic test was performed to provide simulation of moving antenna like a boat or buoy floated on the sea surface. Here, the antenna of a rover station, named ROUT, was driven slowly and simultaneously in both directions horizontal and vertical during observation period for one hour (Fig.3.1). This experiment was repeated every one hour for 4 consecutive days. The data were collected at 1-s time interval. The reference stations ranging approximately from 0.17 – 150 km, namely FIUT (0.17 km), SPRG (30 km), SDNK (60 km), SNAI (90 km), JHBH (100 km), and PGDG (150km) (Fig. 3.2). The satellite elevation cut-off angle was 10 degree. Raw carrier phase and pseudo-range code observations were collected on both the L_1 and L_2 frequencies.

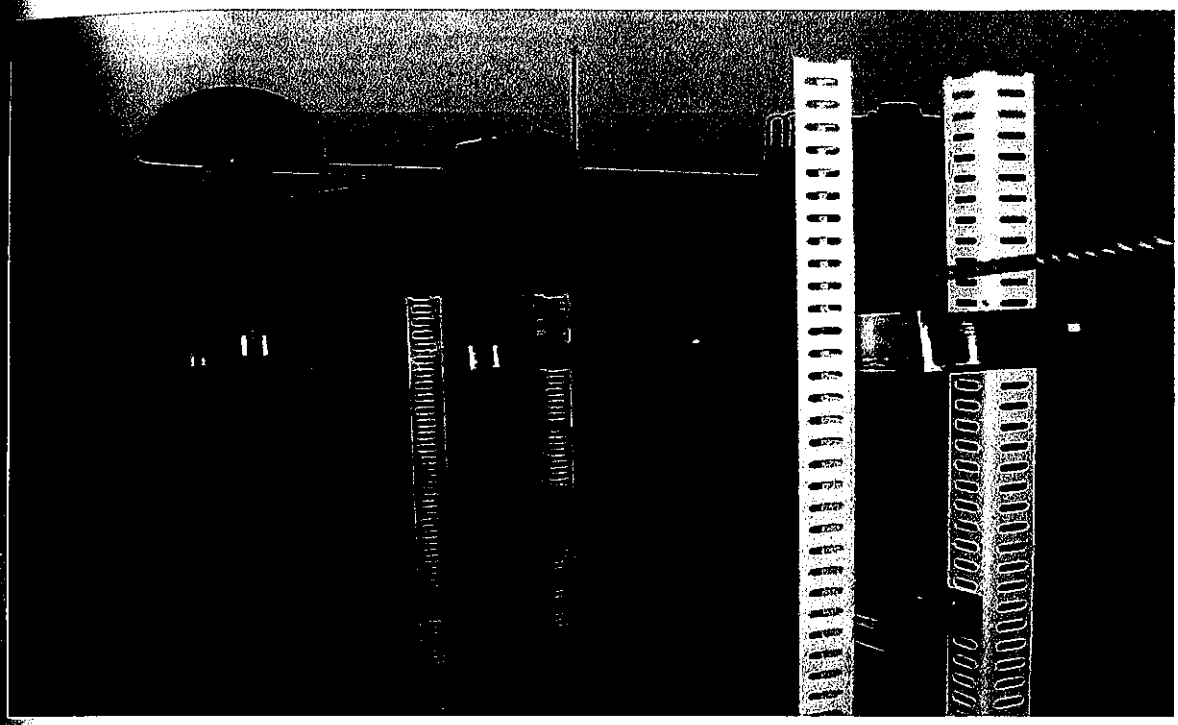

Figure 3.1: An experimental rover station at the roof of the building. Rover antenna down to the slope and is hold up by humans repeatedly for six hours.

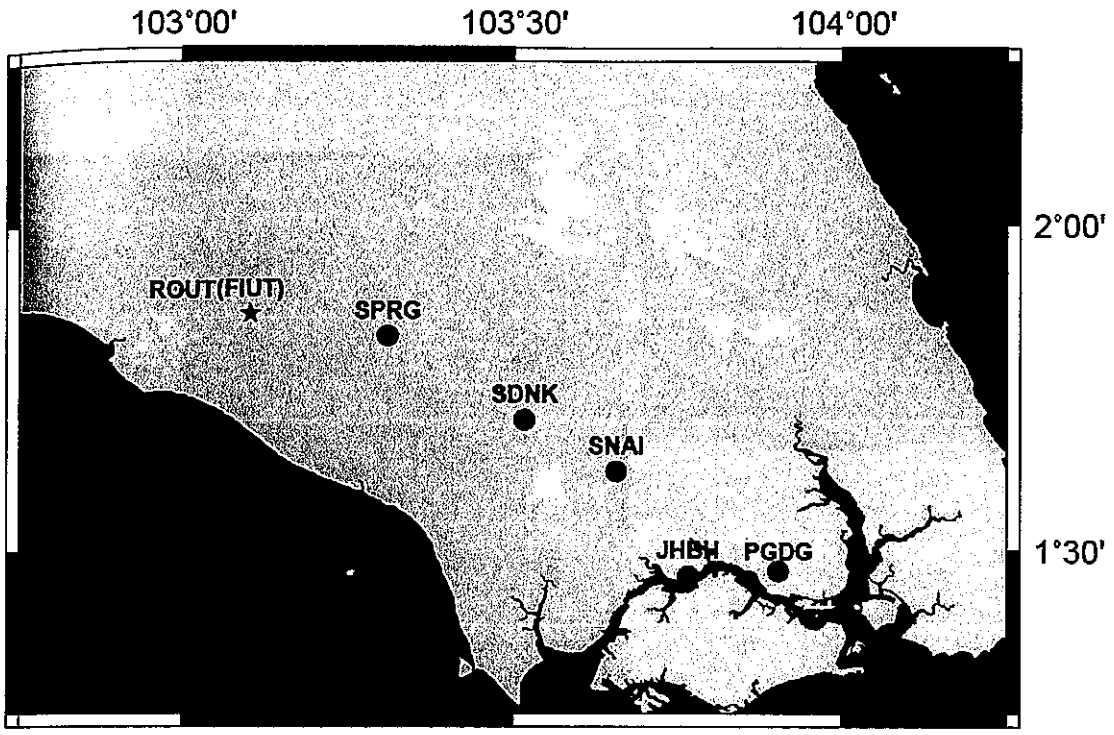

Figure 3.2: Location map of GPS stations for quasi-static kinematic test. Solid circles show the reference GPS stations (SPRG, SDNK, SNAI, and JHBH). The star with solid circle represents the reference baseline between ROUT as a rover and FIUT as a fix station.

3.2.2 Marine Kinematic Test

The marine survey took place in September, 2005 at Kii Peninsula, southwest, Japan (Fig.3.3). A dual-frequency Ashtech Z-12 receiver, connected to an Ashtech choke-ring antenna, was used on the vessel for the survey. The measurements collected by the Ashtech receiver were carrier phase and pseudo-range code on both the L1 and L2 frequencies at 1-second interval. Three base stations HMJM, OWAS, and UGUI stations were used. They are located 300 m, 60 km, and 100 km away from the vessel at the dockside. The vessel remained at dock near HMJM base station for about 800 epochs (about 13 minutes) and then traveled a distance away from the dock. Figure 3.4 illustrates the number of satellites visible in the sky and the satellite geometry during the kinematic survey, as satellite visibility was good in the area of the kinematic survey.

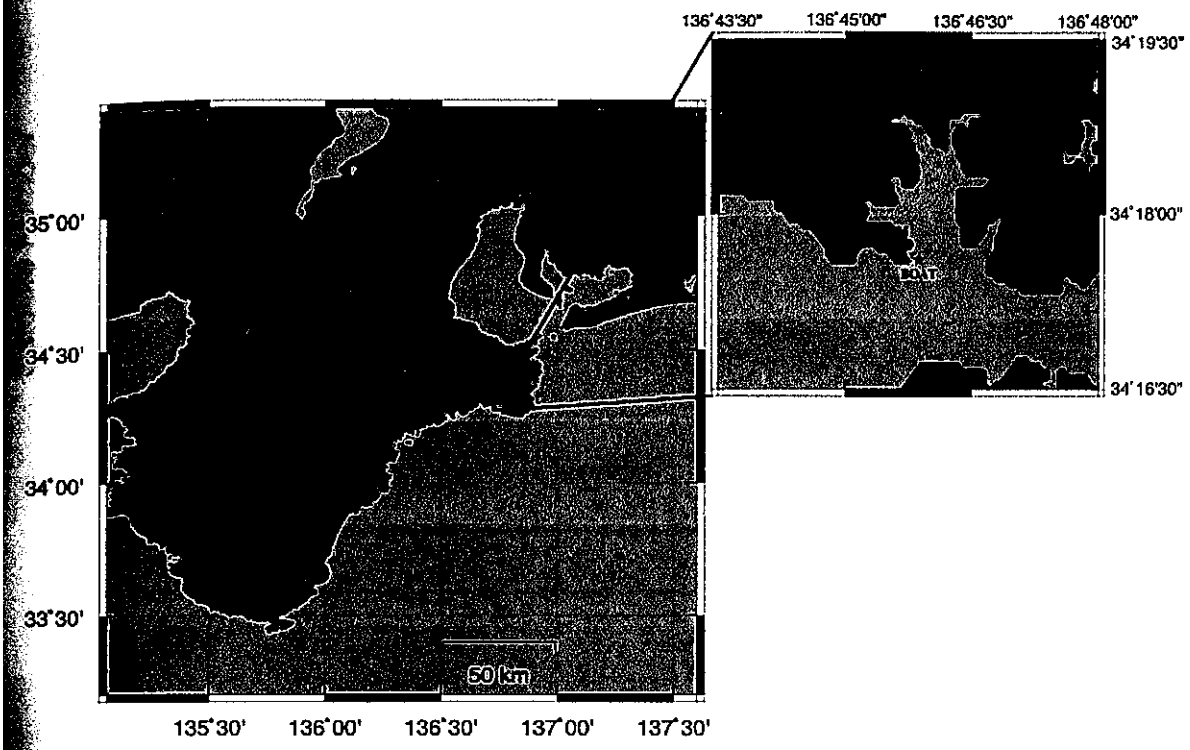

Figure 3.3: Location map of GPS stations for marine GPS survey. Vessel location is shown by star and GPS stations represent by solid circle.

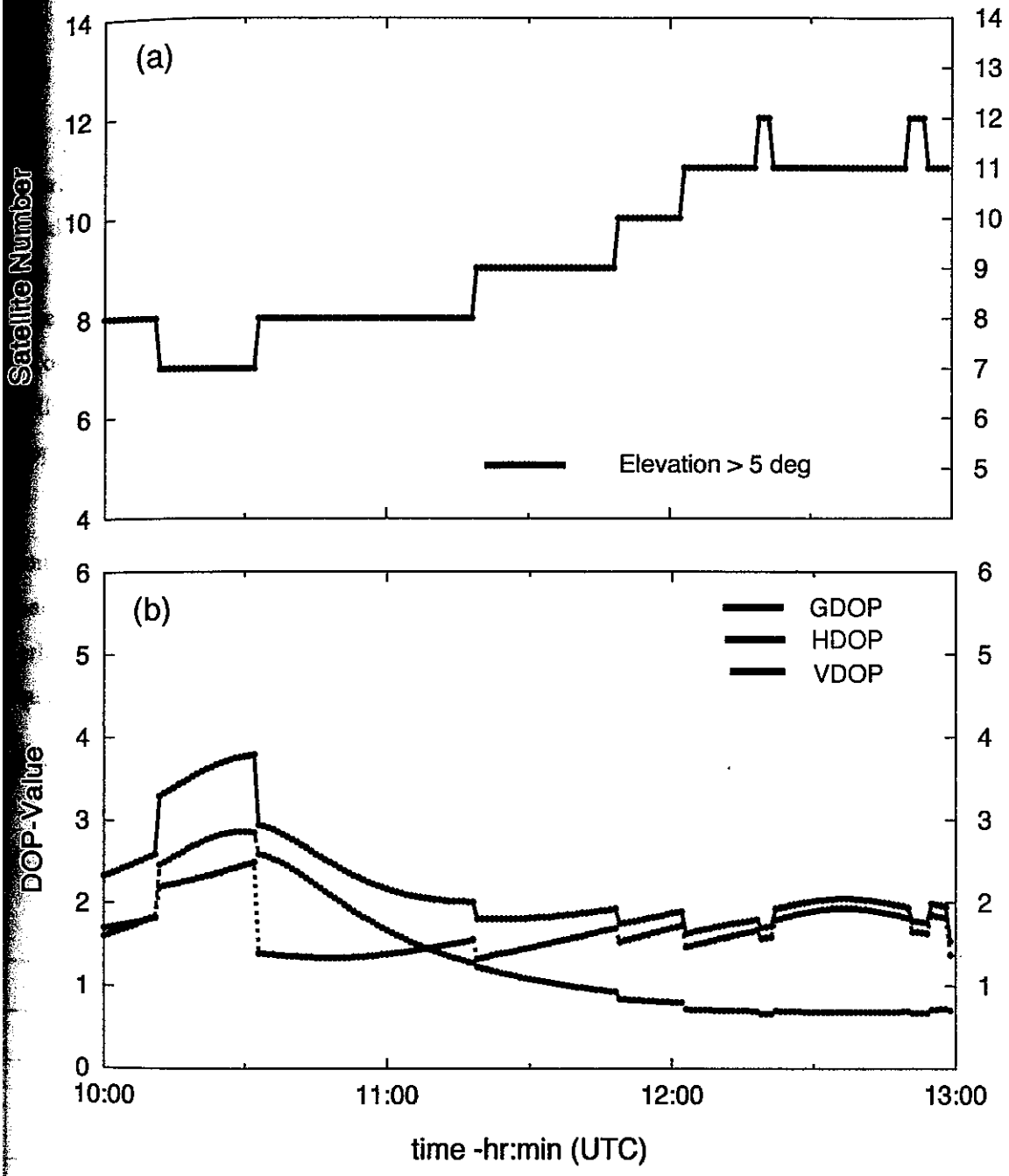

Figure 3.4: Satellite configuration and visibility. (a) Satellite visibilities for 3 hours observations; (b) Dilution of precision values for 3 hours observation.

REFERENCES

Baba, T., K. Hirata and Y. Kaneda, Tsunami magnitudes determined from ocean-bottom pressure gauge data around Japan, *Geophys. Res. Lett.*, **31**, L08303, doi:10.1029/2003/GL019397, 2004.

Born, G. H., M. E. Parke, P. Axerlrad, K. L. Gold, J. Johnson, K. W. Key, D. G. Kubitschek, and E. J. Christensen, Calibration of the TOPEX altimeter using a GPS buoy, J. *Geophys. Res.*, **99**, 24517-24526, 1994.

Bryant, E., Tsunami: The underrated hazard, Cambridge University Press, Cambridge, 2001.

Colombo, O. L., A. G. Evans, M. I. Vigo-Aguir, J. M. Ferrandiz and J. J. Benjamin, Long-baseline (>1000km), sub-decimeter kinematic positioning of buoys at sea, with potential application to deep-sea studies, *ION GPS 2000*, Salt Lake City, 2000.

Effendi Daud M., T. Sagiya, F. Kimata, and T. Kato, Long-baseline quasi-real time kinematic GPS data analysis for tsunami early warning, *Earth Planet Space*, 2008.

Fritz, H. M., W. Kongko, A. Moore, B. McAdoo, J. Goff, C. Harbitz, B. Uslu, N. Kalligeris, D. Suteja, K. Kalsum, V. Titov, A. Gusman, H. Latief, E. Santoso, S. Sujoko, D. Djulkarnaen, H. Sunender, and C. Synolakis, Extreme runup from the 17 July 2006 Java tsunami, *Geophys. Res. Lett.*, **34**, L12602, doi:10.1029/2007/GL029404, 2007.

Georgiadou, Y and A. Kleusberg, On carrier signal multipath effects in relative GPS positioning, Manuscript Geodetica, Vol. 13, No. 3:172-179, 1988.

Gower, J, The 26 December 2004 tsunami measured by satellite altimetry, *Int. J. Remote Sensing*, **28**, *Nos. 13-14*, 2897-2913, 2007.

Han S., Carrier phase-based long-range GPS kinematic postoining. Report from the School of Geomatic Engineering, The University of New South Wales, Australia, 1997

Hassoup, A., Tsunami – A state of the art, National Seismic Network Laboratory, National Research Institute of Astronomy and Geophysics, Cairo, Egypt, 2006.

Hirata, K., H. Takahashi, E. Geist, K. Satake, Y. Tanioka, H. Sugioka, and H. Mikada, Source depth dependence of micro-tsunami recorded with ocean-bottom pressure gauges: the January 28, 2000 Mw 6.8 earthquake off Nemuro peninsula Japan, *Earth Planet Sci. Lett.*, **208**, 305-318, 2003.

Hirata, K., K. Satake, Y. Tanioka, T. Kuragano, Y. Hasegawa, Y. Hayashi, and N. Hamada, The 2004 Indian Ocean tsunami: Tsunami source model from satellite altimetry, *Earth Planets Space*, **58**, 195-201, 2006.

Hoffmann-Wellenhof, B., H. Lictenegger, and J. Collins, GPS:theory and practice. Springer-Verlag, Wien, third edition, 2001.

Hugentobler, U., R. Dach, P. Fridez, M. Meindl, Bernese GPS Software Version 5.0, *Astronomical Institute University of Berne*, 214-219, 2006.

International GNSS Service, http://igscb.jpl.nasa.gov/components/prods.html, 2008.

Kanamori, H., Mechanism of tsunami earthquake, *Phys. Earth Planet Inter.*, **6**, 346-359, 1972.

Kato, T., T. Terada, M. Kinoshita, H. Kakimoto, H. Isshiki, M. Matsuishi, A. Yokoyama and T. Tanno, Real-time observation of tsunami by RTK-GPS, *Earth Planet Space*, **52**, 841-845, 2000.

Kato, T., Y. Terada, M. Kinoshita, H. Kakimoto, H. Isshiki, T. Moriguchi, M. Kanzaki, M. Takada, and J. Johnson, A Development of tsunami observation system using RTK-GPS – Continuous experiment at Ofunato city coast --, Technical Report of IEICE. SANE, 101, 45-52, 2001 (in Japanese with English abstract).

Kato, T., Y. Terada, K. Ito, R. Hattori, T. Abe, T. Miyake, S. Koshimura and T. Nagai, Tsunami due to the 2004 September 5th off the Kii peninsula earthquake, Japan, recorded by a new GPS buoy, *Earth Planet Space*, **57**, 297-301, 2005.